

## A Hydrogen Rearrangement of Formamidine and the Solvent Effects thereupon

K. Yamashita, M. Kaminoyama, T. Yamabe, and K. Fukui

Department of Hydrocarbon Chemistry, Faculty of Engineering, Kyoto University, Kyoto 606, Japan

The nature of the 1,3 hydrogen rearrangement of formamidine ( $\text{H}_2\text{N}-\text{CH}=\text{NH}$ ) and the solvent effects on that reaction are studied with *ab initio* molecular orbital calculations on the basis of the supermolecule model. The reaction path and the motion of the migrating hydrogen atom are traced by using the concept of the intrinsic reaction coordinate (IRC). Four types of orientation of one water molecule to formamidine at the transition state of reaction are examined and the results are discussed from the standpoint of the orbital interactions.

**Key words:** Hydrogen rearrangement – Formamidine – Solvent effects – Intrinsic reaction coordinate.

### 1. Introduction

Hydrogen transfers are involved in many chemical problems and a detailed examination of their mechanism may contribute to a deeper understanding of various general problems of the chemical reactivity. A most important problem on this area may be the proton transfers in biochemical systems and their interaction with environments, such as solvent effects. There are extensive theoretical studies directed toward the solvation of biological as well as general systems [1, 2]. The system to be treated is constituted by a large number of solute and solvent molecules and therefore inevitably some simplifying views are adopted. The existing theoretical approaches are conveniently classified as follows [2]; the pair interactions [3], the supermolecule model [4] and its point charge approximations [5], and the continuum model [6] and closely related supermolecule-continuum model [6].

A sigmatropic hydrogen rearrangement is one of elementary processes involving a hydrogen or proton shift, in which a  $\sigma$ -bond moves across a conjugated system to a new site [7–12]. It is well known that there are two possible modes for the migrating hydrogen; a suprafacial, thermally forbidden process and an antarafacial, thermally allowed process. It should be realized furthermore that the hydrogen shifts occur in the systems involving heteroatoms, the oxygen and/or nitrogen atoms as in biological systems. It would be interesting to study on a major role of heteroatoms in hydrogen rearrangements.

In this study, we performed *ab initio* molecular orbital calculations on the 1,3 hydrogen rearrangement of formamidine,  $\text{H}_2\text{N}-\text{CH}=\text{NH}$ , and on solvent effects for this process. The reaction path and the motion of the migrating hydrogen atom are carefully traced by using the concept of Fukui's intrinsic reaction coordinate (IRC) [13]. The interaction between formamidine and one water molecule are investigated on the basis of the supermolecule model. Various types of orientation of water to formamidine at the transition state are examined and the results are explained in terms of the molecular orbital language.

## 2. Method of Calculations

*Ab initio* MO calculations are carried out by using the HONDO program [14] based on the Hartree–Fock method [15]. The geometry optimization of the transition state as well as tracing of IRC are performed by the energy gradient method [16] with the split-valence 4-31G basis set [17]. The second derivatives of the potential energy surface required for the vibrational analysis at the transition state are obtained by the numerical differentiation of the analytically calculated energy gradient [18].

## 3. Potential Surface for the Hydrogen Shift

### 3.1. Structure of Transition State

Only a single transition state with  $\text{C}_{2v}$  symmetry is found in formamidine. The fully optimized geometry is shown in Fig. 1. The vibrational analysis confirms that this transition state corresponds to a saddle point on the potential energy

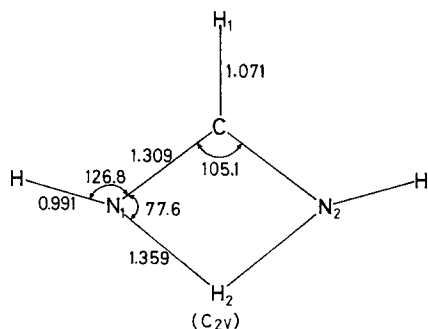
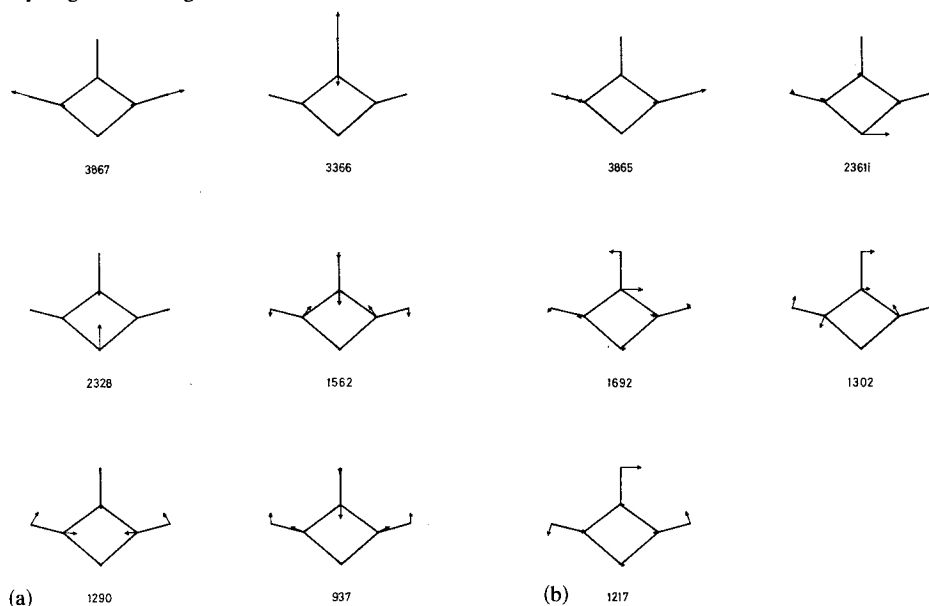


Fig. 1. Fully optimized geometry of transition state (Å, deg.)



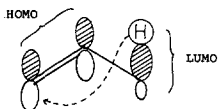
**Fig. 2.** Vibrational frequencies ( $\text{cm}^{-1}$ ) and schematic representations of displacement vectors of normal coordinates at the transition state; (a)  $a_1$  (b)  $b_1$  symmetry

surface, that is, the force constant matrix at this point has one and only one negative eigenvalue [19]. The vibrational frequencies and the displacement vectors of the normal coordinate with  $a_1$  and  $b_1$  symmetry is shown in Fig. 2, whereas for the normal modes with  $a_2$  and  $b_2$  symmetry their vibrational frequencies are only given in Table 1. The normal mode with imaginary frequency has a large amplitude on the migrating hydrogen atom and gives the initial direction of IRC. The IRC starting from this normal coordinate successfully connects the regions of the theoretical reactant  $\text{H}_2\text{N}-\text{CH}=\text{NH}$  and product  $\text{HN}=\text{CH}-\text{NH}_2$ . The converged geometry is that of  $\text{HCNH}$  *cis* isomer, which is reported to be stable than the *trans* isomer by about 2.9 kcal/mol [20]. The analysis along the path will be discussed in the next section. The large imaginary frequency  $2361\text{i cm}^{-1}$  indicates that the potential surface in the vicinity of the transition state would have a steep cliff.

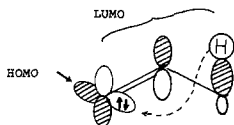
**Table 1.** Calculated vibrational frequencies of normal coordinates with  $a_2$  and  $b_2$  symmetries at the transition state

symmetry	mode	frequency ( $\text{cm}^{-1}$ )
$a_2$	$\nu_{12}$	393
$b_2$	$\nu_{13}$	1282
	$\nu_{14}$	1174
	$\nu_{15}$	750

Sigmatropic rearrangements have attracted considerable theoretical interest, since the advent of orbital symmetry rules [7–12]. It is well accepted that there are two possible modes for the migrating hydrogen atom, a suprafacial, thermally forbidden process and an antarafacial, thermally allowed process. Frontier orbitals well explain these situations for a 1,3-sigmatropic hydrogen shift of propene.



In the cases involving a heteroatom, for example, the keto-enol tautomerism, it is possible to provide a reasonable concerted mechanism for the reaction in addition to the above two paths. The clue lies in the fact that the system involves a heteroatom possessing an occupied  $p$  orbital perpendicular to the  $\pi$ -plane.



A recent *ab initio* calculations actually found two transition states of roughly equal energy for the intramolecular rearrangement of vinyl alcohol to acetaldehyde [21]. These are saddle points of these three possible reaction paths.

In formamidine, the moving hydrogen atom is simultaneously bonded to the terminal atoms  $N_1$  and  $N_2$ . However, both the highest occupied  $\pi$ - and  $\sigma$ -orbitals (corresponding to a combination of the in-plane lone pairs) are antisymmetric with respect to the symmetry plane perpendicular to the molecule. That is, they have  $a_2$  and  $b_2$  symmetries, respectively, and therefore a hydrogen  $1s$  orbital in a planar  $C_{2v}$  structure cannot interact with them. This net antibonding character at the transition state implies that the hydrogen rearrangement in formamidine is a thermally forbidden process. These situations are similar to that in the isoelectronic formic acid system [21].

### 3.2. Analysis along Intrinsic Reaction Coordinate

The potential profile along IRC is shown in Fig. 3. The unit of IRC is (atomic mass unit)<sup>1/2</sup> (bohr). The transition state is located at  $s = 0.0$  and the minus(plus) sign of  $s$  indicates the reactant(product) region of reaction. Due to the symmetry of the system, the right half of the curve is obtained as the mirror image of the left. The reaction is therefore considered to proceed from the left side to the right one.

The calculated barrier 59.1 kcal/mol for this reaction is fairly lower than those for sigmatropic rearrangements of propene (111.7 kcal/mol for antarafacial, 123.9 kcal/mol for suprafacial) [21] and vinyl alcohol to acetaldehyde

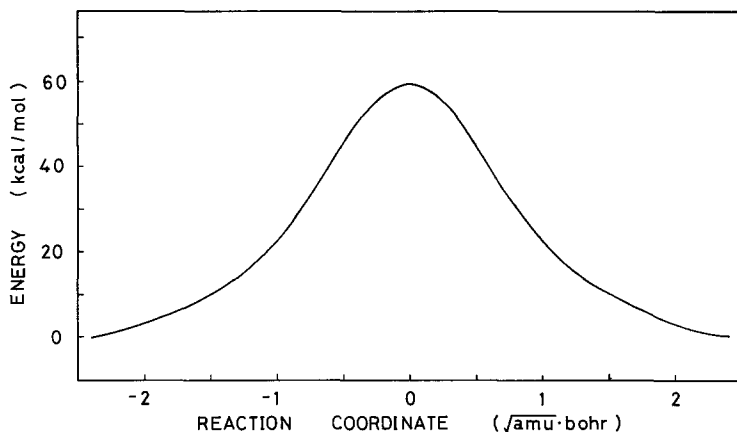


Fig. 3. Potential profile along IRC

(84.6 kcal/mol for antarafacial, 104.8 kcal/mol for suprafacial) [21]. The isoelectronic system, the hydrogen rearrangement of formic acid, gives a similar potential barrier (61.1 kcal/mol) [21].

The motion of the migrating hydrogen along IRC is schematically shown in Fig. 4. The numbers 1, 2, 3 means respectively the position of the reactant, transition state, and product. The migrating hydrogen moves on the molecular plane during the course of reaction. At the initial stage of reaction ( $s = -2.4 \sim -1.2$ ) the bond distance between the migrating atom and the nitrogen  $N_1$  atom does not change so remarkably. The hydrogen atom moves subsequently to the direction of that the  $N_1H$  bond becomes longer. These circumstances would be more understandable by analyzing the changes of the displacement vectors of IRC which give the direction of the motion of constituting atoms along IRC (shown in Fig. 5).

At the reactant, the IRC corresponds to the mode which combines the deformation of the  $NH_2$  group and the deformation of  $NCN$  angle. The component of the deformation of the  $NCN$  angle becomes small with the progress of reaction,

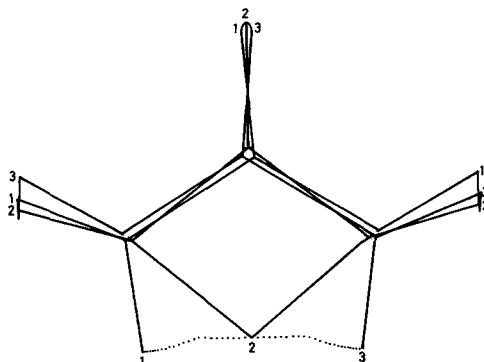
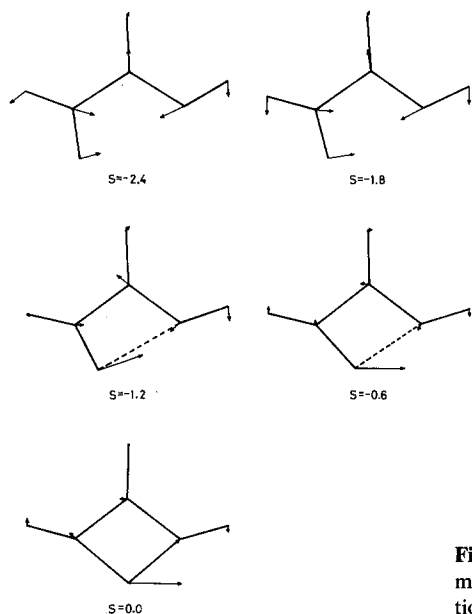


Fig. 4. Motion of the migrating hydrogen atom along IRC; (1) reactant (2) transition state (3) product



**Fig. 5.** Schematic representations of the displacement vector along IRC; (reactant)  $s = -2.4$  (transition state)  $s = 0.0$

and at  $s = -1.2$  the component of the NH bond stretching appears on the migrating atom. The energy about 20 kcal/mol is required for the above process (see also Fig. 3). Two thirds of the potential barrier energy are therefore spent in the process from the point of  $s = -1.2$  to the transition state, where the main component of IRC is the NH bond stretching.

The total gross populations and the net atomic charges at the reactant and the transition state are given in Table 2 (by STO-3G). The charge on the migrating

**Table 2.** New atomic charges ( $q$ ) and total gross population in atomic orbitals at reactant and transition state

	<i>C</i>	<i>N</i> <sub>1</sub>	<i>N</i> <sub>2</sub>	<i>H</i> <sub>1</sub>	<i>H</i> <sub>2</sub>
reactant					
<i>q</i>	0.189	-0.440	-0.387	0.065	0.219
<i>s</i>	3.061	3.409	3.614	0.935	0.781
<i>p</i> <sub>x</sub>	0.950	1.107	1.556		
<i>p</i> <sub>y</sub>	0.931	1.846	1.223		
<i>p</i> <sub>z</sub>	0.869	1.078	0.994		
transition state					
<i>q</i>	0.200	-0.458	-0.458	0.076	0.302
<i>s</i>	3.092	3.532	3.532	0.924	0.698
<i>p</i> <sub>x</sub>	0.962	1.301	1.301		
<i>p</i> <sub>y</sub>	0.823	1.588	1.588		
<i>p</i> <sub>z</sub>	0.923	1.037	1.037		

hydrogen decreases by about  $0.083e$  at the transition state, and this process is less protonic than expected. For the nitrogen atoms, the decrease of the density on the  $p$  AO on the molecular plane is supplied by the increase of the density on that perpendicular to the plane, and results in no change of the charges on these nitrogen atoms.

#### 4. Solvent Effects in the Hydrogen Shift

A most important matter to consider in connection with the influence of solvent on chemical reactions may be the possibility of solvation of the transition state molecule (the molecule at the transition state of reaction). Solvation of the transition state molecule lower the maximum of the potential curve by an amount equal to the heat of solvation and therefore will tend to bring about an increase in the reaction rate, provided that no other factors enter which have an appreciable influence on the potential barrier to the reaction.

Accordingly, we first investigate the solvent effects of formamide at the transition state of the hydrogen shift within the supermolecule model. The interaction potential for the approach of one water molecule to formamide at the transition state are obtained by calculating the energy of the system as a function of the distance,  $R$ , between the migrating hydrogen atom and the oxygen atom of water. The nuclei of formamide and the water molecule are fixed stationary during the water approach along the molecular axis formamide. Four types of the water approach are examined; the water molecule is held on the molecular plane of formamide (A) and then rotated by  $90^\circ$  around the molecular axis of formamide (B), whereas the water is on the plane perpendicular to the molecular axis (C) and rotated by  $90^\circ$  (D). The potential minimum occurs at

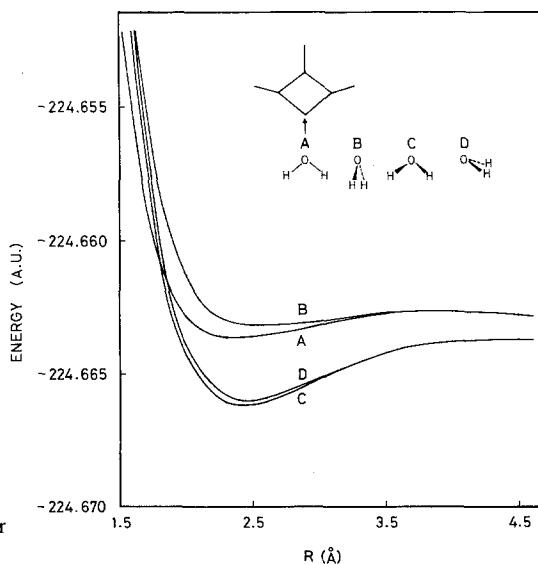


Fig. 6. Interaction potential for the water approach

**Table 3.** Total energies of formamidine and supermolecule and heat of solvation

	Total energy (hartree)	Heat of solvation (kcal/mol)
formamidine		
reactant	-148.8507	—
transition state	-148.7565	—
supermolecule		
$R = \infty$	-224.6639	0.0
<i>A</i>	-224.6636	-0.2
	(-224.6652) <sup>a</sup>	(0.8) <sup>a</sup>
<i>B</i>	-224.6632	-0.4
<i>C</i>	-224.6662	1.4
<i>D</i>	-224.6660	1.3

<sup>a</sup> The geometry of the supermolecule is fully optimized.

approximately  $R = 2.5 \text{ \AA}$  and the potential barrier is less than 1.0 kcal/mol in each case (see Fig. 6). The total energies of these systems decrease in the order of  $C > D > A > B$  as indicated in Table 3. The minus sign of the heat of solvation means that no stabilization of the transition state is obtained. A full geometry optimization of supermolecule using the energy gradient method stabilizes the type *A* held in a  $C_{2v}$  structure about 1.0 kcal/mol. A more 1.0 kcal/mol stabilization energy would be expected in each type if we perform a full optimization of the supermolecule.

Analyses of the molecular orbitals reveal some interesting relationships between these energetics and the types of water approach. The interaction between the formamidine at the transition state and the water molecule is considered as the one of the donor and acceptor interactions (the charge transfer interaction between the lone pair of water and the antibonding  $\text{NH}^*$  MO) and therefore the water HOMO and the formamidine LUMO play an important role. The water HOMO ( $\text{HOMO}_1$ ) and the next one ( $\text{HOMO}_2$ ) are the lone pair MOs lying respectively perpendicular to the molecular plane of water and on the plane. The formamidine LUMO ( $\text{LUMO}_1$ ) is a  $\pi^*$  MO whereas the next LUMO ( $\text{LUMO}_2$ ) is a  $\sigma_{\text{NH}}^*$  orbital. A variety of orbital interactions are therefore born according to the orientation of water formamidine. Their interaction schemes are represented in Fig. 7 where a solid line indicates that the interaction associated with the most important  $\text{LUMO}_2$ . As it is well known, based on the second order perturbation theory [22], the larger the magnitude of the overlapping and the smaller the energy difference between the orbitals considered, the larger is the stabilization energy which is associated with the interaction between them. Considering the orbital energy difference, the interaction between  $\text{HOMO}_1$  and  $\text{LUMO}_2$  is more contributive to stabilization of system than that between  $\text{HOMO}_2$  and  $\text{LUMO}_2$ . The difference in solvation energy between types *C* and



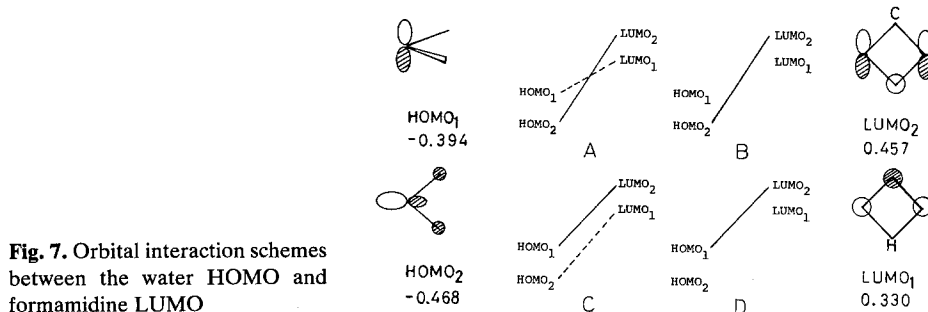


**Fig. 7.** Orbital interaction schemes between the water HOMO and formamidine LUMO

*D* (*A* and *B*) is attributed to the lacking of the HOMO<sub>2</sub>—LUMO<sub>1</sub> (HOMO<sub>1</sub>—LUMO<sub>1</sub>) interaction. It is therefore explained that the type *C* is the most stable form in terms of the molecular orbital language. We can further make an interesting discussion on guanidine, C(NH<sub>2</sub>)<sub>2</sub>NH in which the hydrogen atom bonded to the carbon atom of formamidine is substituted by the NH<sub>2</sub> group. At the equilibrium point of guanidine, the LUMO<sub>1</sub> is the σ<sub>NH</sub><sup>\*</sup> orbital and the LUMO<sub>2</sub> is the π<sup>\*</sup>MO contrary to the case of formamidine [23]. Accordingly, a larger solvation energy is expected for the guanidine and water system, where the type *C* also may be preferable interaction form, provided that the order of these orbitals does not change along the reaction path as in the case of formamidine.

## 5. Concluding Remarks

We have studied the solvent effects at the transition state of the hydrogen migration of formamidine within the supermolecule model. The differences in solvation energy resulting from the types of water orientation to formamidine are well explained in terms of the orbital interaction.

Full geometry optimizations of supermolecule, which have been performed only for the type *A* in this study, will give more stabilization energies for other types. The deformation of the transition state geometry, for example, makes possible for the 1s orbital of hydrogen to interact with the HOMOs of formamidine.

A full tracing of the motion of water relative to formamidine along IRC is more interesting in connection with the changes in the orientation of water and in the potential profile. The latter, in particular, effects the reaction rate through the tunneling of hydrogen atom assisted by solvent effects.

Further study on these points will be reported in future.

*Acknowledgement.* The numerical calculations were carried out at the Data Processing Center of Kyoto University and at the Computer Center of IMS. Financial support was given by the Ministry of Education of Japan (Grand-in-Aid 411106).

## References

1. Clementi, E.: *Lecture Notes in Chemistry*, vol. 2, Berlin and New York: Springer-Verlag, 1976
2. Carsky, P., & Urban, M.: *Lecture Notes in Chemistry*, vol. 16, Berlin and New York: Springer-Verlag 1980
3. Kebarle, P.: *Ann. Rev. Phys. Chem.*, **28**, 445 (1977)
4. Clementi, E.: *Lecture Notes in Chemistry*, vol. 19, Berlin and New York: Springer-Verlag, 1980
5. Scrocco, E., & Tomasi, J.: *Adv. Quant. Chem.*, **11**, 115 (1978)
6. Claverie, P., Daudey, J. P., Langlet, J., Pullman, B., Piazzola, D. & Huron, M. J.: *J. Phys. Chem.*, **82**, 405 (1978)
7. Woodward, R. B. & Hoffman, R.: *Angew. Chem. Int. Ed. Engl.*, **8**, 781 (1961).
8. Fukui, K.: *Acc. Chem. Res.*, **4**, 57 (1971).
9. Klopman, G. ed. G. Klopman. "Chemical reactivity and reaction path", New York: Wiley, 1974
10. Fleming, I.: "Frontier Orbitals and Organic Chemical Reactions", New York: Wiley 1976
11. Pearson, R. G.: "Symmetry rules for chemical reactions. Orbital topology and elementary process", New York: Wiley 1976
12. Epiotis, N. D.: *Concepts in Organic Chemistry*, vol. 5, Berlin and New York: Springer-Verlag 1978
13. Fukui, K.: *J. Phys.. Chem.*, **74**, 4161 (1970)
14. Dupuis, M., King, H. F.: *J. Chem. Phys.*, **68**, 3998 (1978)
15. Roothaan, C. C. J.: *Rev. Mod. Rhys.*, **23**, 69 (1951)
16. McIver, J. W. Komornicki, A.: *Chem. Phys. Lett.*, **10**, 303, (1971); Komornicki, A., Ishida, K., Morokuma, K., Ditchfield, R., Conrad, M.: *Chem. Phys. Lett.*, **45**, 595 (1977)
17. Ditchfield, R., Hehre, W. J., Pople, J. A.: *J. Chem. Phys.*, **54**, 724 (1971)
18. Pulay, P.: ed. H. F. Schaefer III, in "Modern theoretical chemistry", vol. 4. New York: Plenum, 1977
19. McIver, J. W., Komornicki, A.: *J. Am. Chem. Soc.*, **94**, 2625 (1972); Poppinger, D.: *Chem. Phys. Lett.*, **35**, 550 (1975).
20. Radom, L., Hehre, H. J., Pople, J. A.: *J. Am. Chem. Soc.*, **93**, 289 (1971); Ditchfield, R., Delbene, J. F., Pople, J. A.: *J. Am. Chem. Soc.*, **94**, 703 (1972)
21. Bouma, W. J., Vincent, M. A. Radom, L.: *Int. J. Quant. Chem.*, **14**, 767 (1978).
22. Fukui, K.: "Theory of orientation and stereoselection", Berlin and New York: Springer-Verlag 1975
23. Kollman, P., Mckelvey, J., Gund, P.: *J. Am. Chem. Soc.*, **97**, 1640 (1975)

Received July 13, 1981